The ebb and flow of protons: A novel approach for the assessment of estuarine and coastal acidification
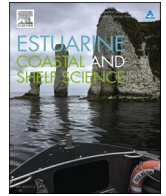
5 authors, including:

Stephen Gonski
University of Delaware
5 PUBLICATIONS **16** CITATIONS

SEE PROFILE

ELSEVIER

The ebb and flow of protons: A novel approach for the assessment of estuarine and coastal acidification

D. Tye Pettay [a,b,*], Stephen F. Gonski [c,d], Wei-Jun Cai [d], Christopher K. Sommerfield, [†a,1], William J. Ullman [a]

[a] *School of Marine Science and Policy, University of Delaware, Lewes, DE, USA*
[b] *Department of Natural Sciences, University of South Carolina Beaufort, Beaufort, SC, USA*
[c] *Washington State Department of Ecology, Olympia, WA, USA*
[d] *School of Marine Science and Policy, University of Delaware Newark, DE, USA*

ARTICLE INFO

ABSTRACT

The acidification of estuarine and coastal waters is a consequence of both natural (e.g., aerobic respiration) and anthropogenic (e.g., combustion of fossil fuels, eutrophication) processes and can negatively impact the surrounding ecosystems. Until recently it was difficult to accurately measure pH, and thus total proton concentrations ($[H_T^+]$), when salinities vary significantly and rapidly as a consequence of tidal mixing. Proton production and transport are ultimately responsible for acidification in nearshore environments, and the uncertainty surrounding proton concentrations measured at high frequency has hindered our understanding of the net impact of global and local processes on estuarine and coastal acidification. Here, we quantify the rate of proton exchange between an estuary and bay to assess the extent of acidification by using the novel combination of high frequency pH_T (total hydrogen ion concentration scale) data from an autonomous SeapHOx™ sensor and continuous tidal discharge measurements made between the eutrophic Murderkill Estuary and Delaware Bay. Proton fluxes reverse with each tide. However, the net non-tidal proton fluxes are directed upstream and display seasonal changes in magnitude. Our results indicate that Delaware Bay contributes to the acidification of the Murderkill Estuary, yet the degree of acidification is reduced in the summer. Using proton concentrations measured at high temporal resolution to calculate proton fluxes provides a new and relatively simple approach for quantifying the acidification of dynamic nearshore environments.

1. Introduction

Acidification of natural waters represents a net increase in hydrogen ion concentration ($[H^+]$ or "protons") that is dependent on changes in the magnitude of proton-producing and -consuming processes (Hoffman et al. 2009). Open-ocean acidification, due primarily to the dissolution of atmospheric CO_2 into seawater to produce carbonic acid (H_2CO_3), progresses at approximately the same rate around the world (-0.001-0.002 pH units year^{-1}), while the rates in estuaries and the coastal ocean are consistently estimated to be an order of magnitude higher (Provost et al. 2010; Duarte et al. 2013Bates et al., 2014; Carstensen and Duarte, 2019). In estuarine and coastal waters carbon dioxide (CO_2) dissolution combines with local eutrophication and the aerobic respiration of allochthonous and autochthonous organic matter

to enhance acidification (Sunda and Cai, 2012; Wallace et al. 2014). As the delivery of nutrients and organic carbon to estuaries and coastal waters increases, higher rates of local acidification are anticipated (Feely et al., 2010; Cai et al. 2011; Wallace et al. 2014). Conversely, biological processes, such as primary production and mineral dissolution, moderate acidification by consuming CO_2 (Borges and Gypens, 2010; Aufdenkampe et al. 2011; Duarte et al. 2013). Due to the large number of competing acid-consuming and -producing processes and environmental proton sources and sinks, it is challenging to determine the net rates of all of the processes that contribute to and mitigate the acidification of any particular water body (Hofmann et al. 2010 and the references therein).

Proton cycling is the sum of all proton-consuming and -producing processes within a body of water. In an estuary, this cycling is influenced
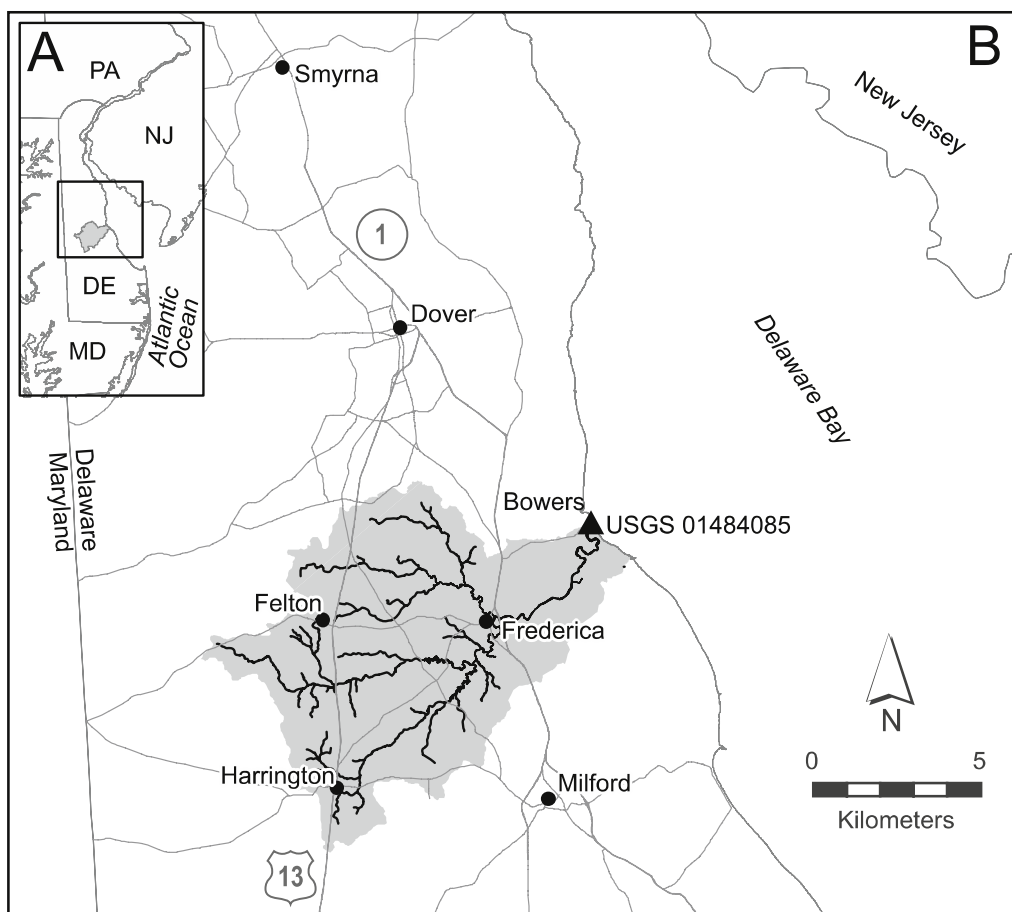
---

by a number of hydrophysical and hydrochemical processes. In general, proton concentrations are elevated (lower pH; pH = $-log[\text{H}_T^+]$) in the upper watershed and around marshes due to freshwater inputs, respiration and nitrification. These elevated concentrations flow downstream on the ebb tide and into the nearshore coastal waters where protons are consumed by primary production and CO_2 degassing and, together with dilution and carbonate buffering, cause proton concentrations in the waters of the returning flood tide to decline (pH increases; Cai et al. 2000; Wang and Cai, 2004; Hofmann et al. 2009).

The imbalance between proton sources and sinks explicitly leads to long-term changes in acidity and is highly variable among coastal systems. The research community has recognized this fact and is transitioning towards the inclusion and analysis of proton concentrations when characterizing acidification in estuarine, coastal and oceanic waters (Hofmann et al. 2010; Fassbender et al. 2017; Kwiatkowski and Orr, 2018). The determination of proton production, consumption, and transport is needed to assess: (1) whether a particular water body will become acidified; (2) the rate and extent of acid production and consumption within the water body; and (3) the rates and direction of proton exchange between adjacent and connected water bodies. Measured proton fluxes can help address this need by quantifying the rates of proton cycling and the direction of acidification within nearshore waters. Changes in carbonate chemistry (dissolved inorganic carbon; DIC and total alkalinity; TA) are commonly used to calculate pH and to determine the rates of biogeochemical processes leading to the acidification of natural waters. However, this approach is time consuming, tedious, and rarely capable of producing pH measurements over the temporal and spatial scales that approximate the inherent variability of physically and biogeochemically dynamic coastal waters (see Section 3.1 for further discussion; Hofmann et al. 2008; Hofmann et al. 2010). Recent advances in pH sensor technology bridge this gap and now provide the opportunity to calculate the flux of protons between water bodies, an innovative approach to assess acidification.

To date, we are aware of only one estuarine system, the Scheldt Estuary, for which the notion of proton cycling has been considered, where the net consumption of protons (modeled at 20 kmol y^{-1} for the whole estuary) has already resulted in a gradual increase in estuarine surface pH over time (Borges and Gypens, 2010; Hofmann et al. 2009). While proton fluxes have been discussed in coral reef systems and analyzed on a global scale relative to changes in $p\text{CO}_2$ (e.g., Jokiel, 2016; Fassbender et al. 2017), similar quantification of net proton fluxes within and between estuarine water bodies, as was done in the Scheldt, is not available. However, quantification of these fluxes can help determine the ultimate impact of acidification on ecosystems and ecological processes, and to develop practical and scalable mitigation strategies for acidification-dependent environmental degradation. Here we report measured proton concentrations and calculated fluxes within a dynamic estuarine environment (the confluence of eutrophic Murderkill Estuary and Delaware Bay, Delaware, USA; Fig. 1). The instantaneous fluxes were determined for the biologically productive Spring and Summer months in 2016, using high frequency pH data from a SeaPHOx™ sensor and discharge measurements at a US Geological Survey (USGS) gaging station. Agricultural runoff and discharge from a wastewater treatment plant significantly influence water quality within the Murderkill Estuary. As a consequence of these inputs, (1) nutrient concentrations are elevated in the upper Murderkill Estuary; (2) the estuary experiences

Fig. 1. Map of the Murderkill Watershed and sensor location. Location of the Murderkill Watershed in the Mid-Atlantic and state of Delaware (A, inset). The Murderkill Watershed (grey) and the USGS gauging station (DE01484085) in Bowers, Delaware (triangle) at the confluence of the Murderkill Estuary and Delaware bay (B). An autonomous pH sensor was co-located at the USGS gauging station during the Spring and Summer of 2016.

hypoxia during the summer months; and (3) nitrogen and phosphorus burial rates in the adjacent marsh sediments have increased two-fold since the mid-1970s (DNREC, 2014Velinsky et al. 2010). Therefore, this eutrophic estuary makes an ideal case study to quantify the influence of proton cycling and exchange on the coastal ocean.

2. Materials and methods

2.1. Site description

The Murderkill Watershed and Estuary are located in southeastern Kent County, Delaware (Fig. 1). The 342 km^2 watershed is predominantly agricultural (56%), with lower fractions of urban (16%), forested (11%), and wetlands (including forested wetlands, 17%) land-uses (Ullman et al. 2013). The watershed has well-drained soils, consistent with its coastal plain setting (Andres, 2004). Most of the rural development in the watershed disposes of its wastewater through domestic septic and small community systems (DNREC, 2006). However, the Kent County Regional Resource Recovery Facility (KCRRRF) that discharges to the upper Murderkill Estuary treats wastewater originating from both within and outside the watershed, including the nearby urban centers of Dover, Smyrna, and Milford, Delaware (Fig. 1). Discharge from the KCRRRF increases the effective anthropogenic pressure on the Estuary and its downstream waters. The Murderkill Estuary has an average width of 50 m and an average channel depth of 4.5 m, and discharges to Delaware Bay at Bowers, Delaware, approximately 39 km upstream of the Delaware Bay mouth, where it supports high and persistent levels of primary production in the Bay margins during the summer months (Wong et al. 2009; Voynova et al. 2015). Delaware Bay drains a 36,570 km^2 watershed that encompasses parts of Delaware, New Jersey, Pennsylvania, and New York State with the tidal portion extending 215 km into New Jersey and Pennsylvania (Voynova et al. 2015). The width of the Bay increases from about 18 km at the mouth to about 44 km upstream and has a mean depth of 6 m (Sharp et al. 2009; Wong et al. 2009). The Delaware and the Schuylkill Rivers provide more than 70% of the freshwater flow into the Bay, but numerous small tributaries, including the Murderkill River, discharge along the margins of the bay and contribute significant nutrient loads to the Bay (Voynova and Sharp, 2012; Voynova et al. 2015). Discharge through the River/Bay is typically higher in the Spring than the Summer, however, in 2016 the Spring was drier than the Summer by ~30 mm in precipitation for the Murderkill Estuary (data from Kitts Hummock National Estuarine Research Reserve (NERR) station < nerrsdata.org/get/realTime.cfm?stationCode 1/4 DELSJMET>; approximately 5 km northwest of Bowers). Temperature, salinity and pH are temporally and tidally variable in both the Murderkill River and Delaware Bay, with ranges for the River/Bay system of ~0 – 33 °C, 3 – 30 g/kg and 6.5 – 8.3, respectively (Ullman et al. 2013; Voynova et al. 2015; Gonski et al. 2018).

2.2. Instrumentation

The SeapHOx sensor package is integrated with sensors for temperature, salinity (Sea-Bird Electronics Conductivity-Temperature Sensor – SBE37), pH (Honeywell Durafet), and oxygen (Aanderaa Data Instruments 4835 Optode) deploying in sequence as water is pumped through the sensor flow path by a Sea-Bird Electronics 5M submersible pump (Bresnahan et al., 2014). The SeapHOx was deployed at the confluence of the Murderkill Estuary and Delaware Bay where it sampled waters discharging from the Estuary to the Bay on falling tides and waters recharging the Estuary from the Bay on rising tides. The SeapHOx was deployed adjacent to the main tidal channel of the Estuary at approximately 1 m above the estuarine floor and 3 m below mean high tide. During the Spring (12 May to 09 June) and Summer (20 July to 24 August) 2016, the sensor measured pH$_T$, temperature, and salinity every 30 min. Due to sedimentation and biofouling, the instrument was cleaned and serviced at intervals of 1–2 weeks and data were not

collected during the servicing periods when the instrument was out of the water (described by Gonski et al. 2018). The US Geological Survey operates a tidal gauging station at this site (USGS 01484085), in cooperation with the Delaware Geological Survey and the State of Delaware. Consistent with the USGS convention, positive discharges and fluxes are directed downstream. Co-located with these instruments was a Seabird Scientific Land Ocean Biogeochemical Observatory that provides additional biogeochemical data (not reported here) for both the Murderkill Estuary and Delaware Bay depending on the direction of tidal flow (Voynova et al., 2015).

2.3. SeapHOx calibration

The Honeywell Durafet and its integrated reference electrodes, built into the SeapHOx sensor, calculate and report a pair of pH values on the total scale (pH$_T$): pH^{INT} (internal reference, Ag/AgCl reference electrode containing a 4.5 KCl gel liquid junction, FET|INT) and pH^{EXT} (external reference, solid-state chloride ion-selective electrode, Cl-ISE, FET|EXT). The SeapHOx was calibrated using an *in situ* or field calibration procedure where discrete bottle samples were collected in the field for laboratory analysis of DIC and TA alongside simultaneous SeapHOx sensor measurements. Duplicate bottle samples were collected for DIC and TA analysis in triple-rinsed, 250-mL borosilicate glass bottles by bottom-filling and overflowing following filtration through Whatman 0.45 mm Polyethersulfone (PES) filters (GE Healthcare Bio-Sciences, Pittsburgh, PA, USA). The calibration samples were fixed with 100 μL of saturated mercuric chloride (HgCl$_2$), securely closed, and stored on ice and in the dark at ~4 °C until returned to the laboratory for analysis (Cai and Wang, 1998; Huang et al. 2012). Calibration samples for the Spring (N = 21) and Summer (N = 24) pH time-series were collected every 30 min on 01 June 2016 and 02 August 2016, respectively, over full tidal cycles to capture the entire salinity range observed on those days (Gonski et al. 2018). DIC was determined in the laboratory, as CO$_2$ gas, using a non-dispersive infrared gas analyzer following sample acidification (AS-C3 Apollo SciTech). TA was determined by Gran Titration (Gran, 1950, 1952) using a semi-automated open-cell titration system (AS-ALK2 Apollo SciTech) (Cai et al. 2010; Huang et al. 2012; Wang and Cai, 2004). Both instruments were calibrated using certified reference materials (CRMs), provided by A.G. Dickson (Scripps Institution of Oceanography), yielding results with a precision of ±2.2 μmol kg^{-1}. A set of reference pH measurements for the calibration samples was calculated on the total scale from measured DIC and TA at *in situ* temperature, salinity, and pressure using the inorganic carbon dissociation constants of Millero et al. (2006), the bisulfate ion acidity constant of Dickson (1990), and the boron-to-chlorinity ratio of Lee et al. (2010) using the Excel macro CO2SYS (Pierrot et al. 2006). The sensor data was then recalibrated to minimize the anomaly between the sensor pH$_T$ and reference pH$_T$ determined from the calibration samples by setting the calibration constants specific to each reference electrode to average values based on all valid calibration samples (Bresnahan et al. 2014).

Using this rigorous calibration scheme, the sensor pH had root-mean-square errors of 0.0275 and 0.0159 pH units for the Spring and Summer periods, respectively, relative to pH$_T$ calculated from measured DIC and TA (Gonski et al. 2018). The pH$_T$ and salinity of calibration samples on 1 June 2016 ranged between 7.1 and 8.3 and 8.99 and 22.31, respectively. On 2 August 2016, pH$_T$ and salinity of calibration samples ranged between 7.0 and 7.9 and 21.07 and 27.06, respectively. In the present work, the pH^{INT} time-series was used for both time periods and calibrated using an *in situ* multi-point calibration approach, which provides a more robust measurement over a wide range of time-varying salinities in estuarine environments (Gonski et al. 2018; Miller et al. 2018). For a more thorough discussion of the sampling approach and sensor calibration, the reader is referred to Gonski et al. (2018).

No corrections were made for possible "excess" (non-carbonate) alkalinity in the calibration samples. This contribution to alkalinity is

not likely to exceed 1–2% of the total alkalinity and therefore should have no significant impact on the SeapHOx calibration (Gonski et al. 2018). The present pH data closely approximates the precision recommended by the Global Ocean Acidification Observing Network (GOA-ON) for weather-level pH measurement precision (Newton et al., 2015), and, as such, are sufficient for resolving the directions and magnitudes of proton fluxes between the Murderkill Estuary and Delaware Bay.

2.4. Time series analysis

Prior to flux calculations, the half-hourly measured continuous pH_T data was interpolated linearly to match the 6-min interval of the discharge measurements. Instantaneous proton concentrations on the total hydrogen ion concentration scale were calculated from the measured values of pH_T and the definition of pH_T:

$$[H_T^+] = 10 \; \hat{} \; (-pH_T)$$

The non-tidal component was separated from the instantaneous time series for discharge and $[H_T^+]$ using a 40-h low-pass Butterworth filter (Ganju et al. 2005; Dzwonkowski et al., 2014). Filtering was performed in R using the 'signal' package (Ligges et al. 2013) with a double-pass filter and n = 3 (i.e., 3rd order), removing all variation due to tidal harmonics. The filtered non-tidal discharge and $[H_T^+]$ were used to calculate net non-tidal fluxes for each sampling period. The instantaneous data for salinity was also linearly interpolated and filtered, as described above, to calculate a salt flux for each period. Salinity represents a conservative constituent and was used to validate the flux calculations. For the purposes of calculating fluxes, salinity was considered to be in units of g kg^{-1}.

2.5. Subsampling of protons

High frequency, continuous monitoring reveals patterns in biogeochemical processes that may be missed using less frequent, single time point sampling typical of historical sampling strategies. To further demonstrate this point we randomly subsampled interpolated proton concentrations from the Spring and compared the distribution of the means of these subsamplings to that of the overall mean. Four hypothetical "sampling" strategies were developed and consisted of random pH measurements taken during 3-h windows (similar to recommended by Skeffington et al. 2015) either in the morning (9:00 to 11:00) or afternoon (14:00 to 16:00) and sampled every other day starting either on day 1 or day 2 of the Spring dataset. These four subsamplings were therefore named day1AM or day1PM, and day2AM or day2PM. A proton concentration was randomly drawn in the morning or afternoon on every other day and a mean was computed from all of these single daily measurements. Each subsampling was repeated 10,000 times and the frequency distributions of the means were plotted against each other and the overall mean for the Spring 2016.

2.6. Flux calculations

Advective fluxes of dissolved material C (J_C) can be calculated as the product of concentration (C, mass/m^3) and discharge (Q, m^3/time) for any period for which instantaneous or integrated C and Q are both available or can be estimated:

$$J_c = (C \times Q)$$

The instantaneous density of seawater, determined using salinity and temperature, was used to convert kg to m^3. The low-pass filtered data for both C and Q were used to calculate the non-tidal fluxes of protons and salt. The mean and standard error (Table 1) were calculated for seasonal discharge measurements and fluxes.

Table 1
Summary of mean Spring and Summer fluxes from the Murderkill Estuary to Delaware Bay in 2016 (±standard error).

Non-Tidal Flux[a]	Spring 2016	Summer 2016
Water	-0.78 ± 0.05 m^3 s^{-1}	-0.40 ± 0.04 m^3 s^{-1}
Salt	-75 ± 3.5 Mg h^{-1}	-48 ± 3.7 Mg h^{-1}
Protons	-9.6 ± 5.5 mmol h^{-1}	-1.3 ± 2.8 mmol h^{-1}

[a] Positive fluxes are directed downstream towards the Bay.
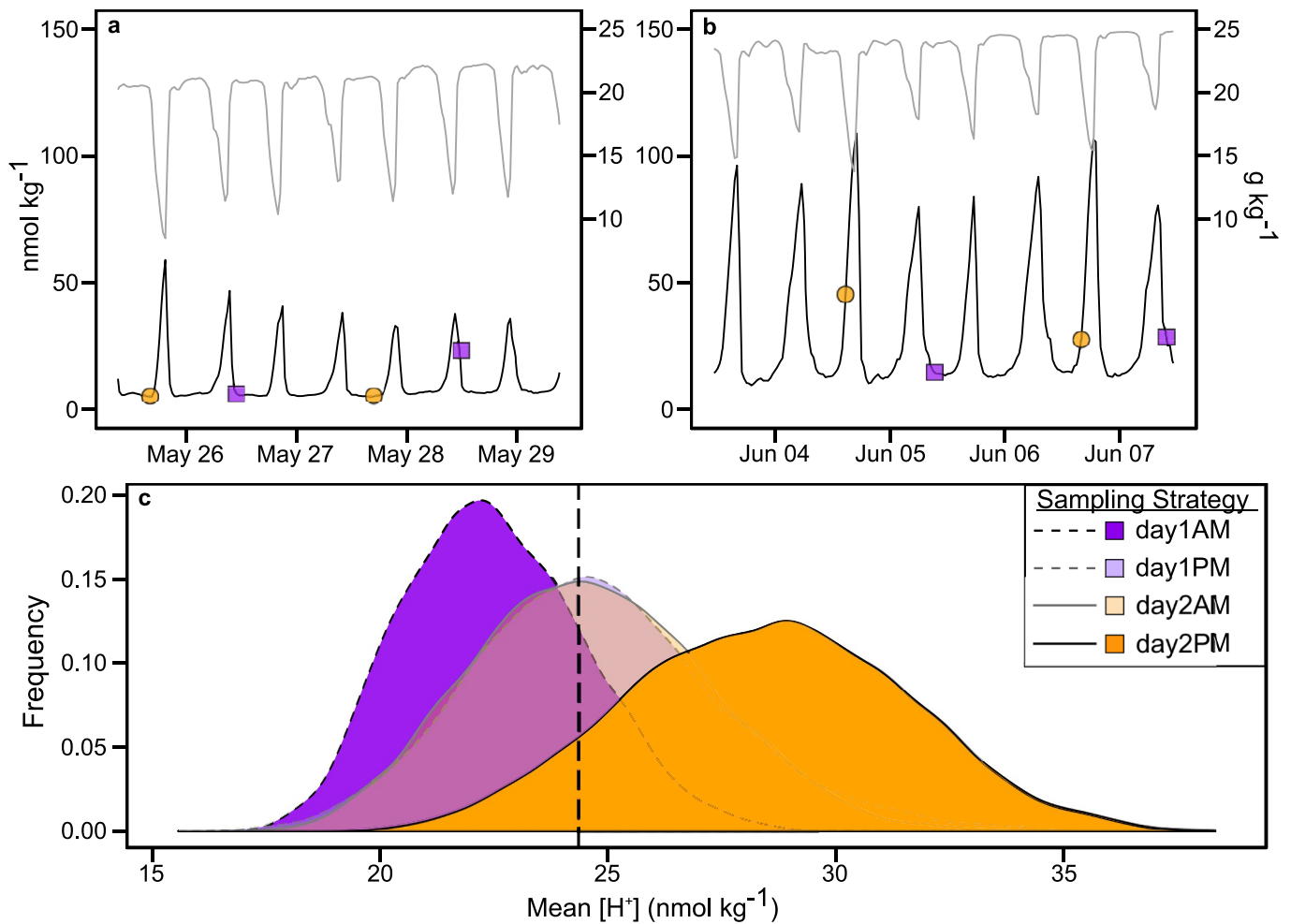
3. Results and discussion

3.1. Measuring protons in dynamic saline environments: Why now?

Previous work has criticized the strong focus on alkalinity changes when characterizing the acid-base chemistry of natural waters (Hofmann et al. 2010), while others have further discussed the limitations of using pH to assess acidification, showing proton concentrations to be a more robust indicator (Fassbender et al. 2017; Kwiatkowski and Orr, 2018). Changes in observed pH actually reflect proton consumption and production by numerous biogeochemical processes, and only indirectly involve alkalinity reactions (Hofmann et al. 2010). These processes are seasonal in nature and geographically variable, and using pH to quantify acidification captures only a small portion of this variability when compared to $[H_T^+]$ (Fassbender et al. 2017, Fassbender et al. 2018a & b, Kwiatkowski and Orr, 2018). In fact, across most latitudes seasonal pH variability is projected to decrease in the future, while proton variability is predicted to significantly increase (Fassbender et al. 2017; Kwiatkowski and Orr, 2018). The differences between these two apparently identical measurements are due to the logarithmic nature of the pH scale and the complexity of the carbonate buffering in estuarine and marine waters. These modeling efforts are extremely informative on a global and regional scale, however they do not explicitly account for or document the high frequency temporal variations that occur within individual coastal systems (Fig. 2). As such, there is a strong need for high frequency, long-term measurements of $[H_T^+]$ across distinct coastal and estuarine systems to better understand shorter-term variability and seasonal differences so that this information can be incorporated into predictive models of ocean acidification (Fassbender et al. 2018).
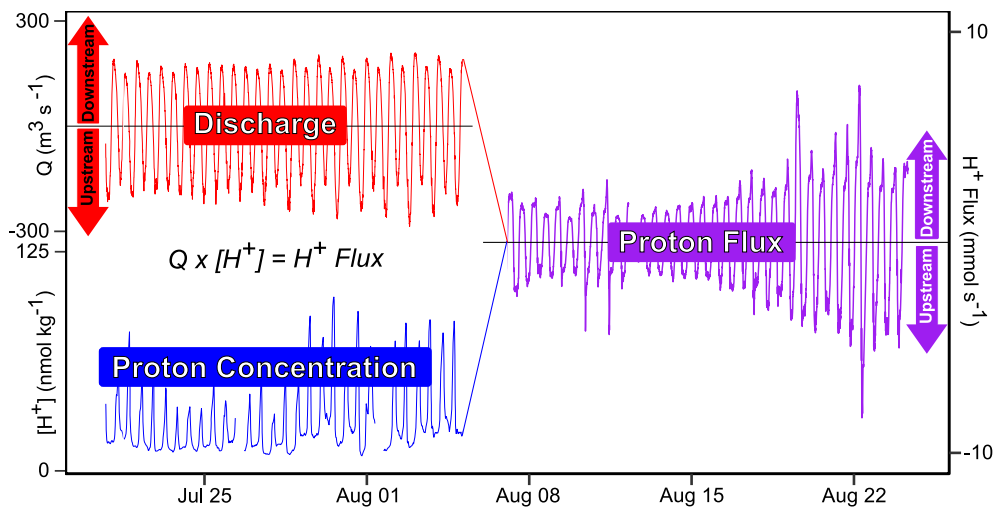
Cation interferences on the performance of *in situ* glass electrodes, together with their slow response time, previously made continuous measurements of pH in estuaries with rapidly varying salinity highly uncertain. This traditional methodology of using glass electrode potentiometry to yield proton activities is subject to unpredictable and irreproducible liquid junction errors in brackish and saline waters (Bates, 1973; Butler et al. 1985; Easley and Byrne, 2012; Whitfield et al. 1985), often making the conversion of proton activity to proton concentration imprecise (Dickson, 1984). Accordingly, glass electrode potentiometry is no longer the preferred methodology in contemporary studies of pH in marine and estuarine waters, unless used with alternative methods of calibration (Easley and Byrne, 2012; Wootton and Pfister, 2012; Martz et al. 2015; Gonski et al. 2018). In seawater, the determination of proton concentrations on the total hydrogen ion concentration scale (pH_T) is now preferred (Dickson, 1984, 1993).

To overcome the above analytical issues, several autonomous biogeochemical sensors built around a proton-sensitive Ion-Selective Field-Effect Transistor (ISFET) were developed to yield more rapid, precise, accurate, and reproducible pH_T measurements in natural waters, including seawater (Bresnahan et al. 2014; Martz et al. 2010). When used with appropriate calibration procedures, these ISFETs are subject to substantially less interference from seawater cations, have smaller "memory" effects, improved long-term stability and respond more rapidly than the glass electrode to changes in ambient proton concentrations in estuarine and marine settings (Martz et al. 2010; Bresnahan et al. 2014; Takeshita et al. 2014; Gonski et al. 2018). Using this recent advance in pH sensor technology, together with appropriate

Fig. 2. A conceptualization of short-term variability in proton concentrations due to tidal forcing based on data collected in Spring 2016. Proton concentrations (black) for both neap (a) and spring (b) tides. Salinity (grey) is plotted as a surrogate for tidal stage, where salinity maxima occur during flood tides and minima occur during slack ebb tides. Colored points (a & b) are examples of randomly sampled time points for day1AM (purple squares) and day2PM (orange circles) only (see Methods for description of subsampling). These points demonstrate real variability missed when sampling at lower frequencies and how different sampling strategies can lead to differing values of mean proton concentration. Frequency distributions of mean proton concentrations based on four subsampling schemes (c); day1AM (black dashed line, purple fill), day1PM (grey dashed line, light purple), day2AM (grey solid line, light orange), day2PM (black solid line, orange), and the overall mean for Spring 2016 (dashed vertical line). Day1PM and day2AM distributions overlap each other and the overall mean for the Spring. (For interpretation of the references to colour in this figure legend, the reader is referred to the Web version of this article.)
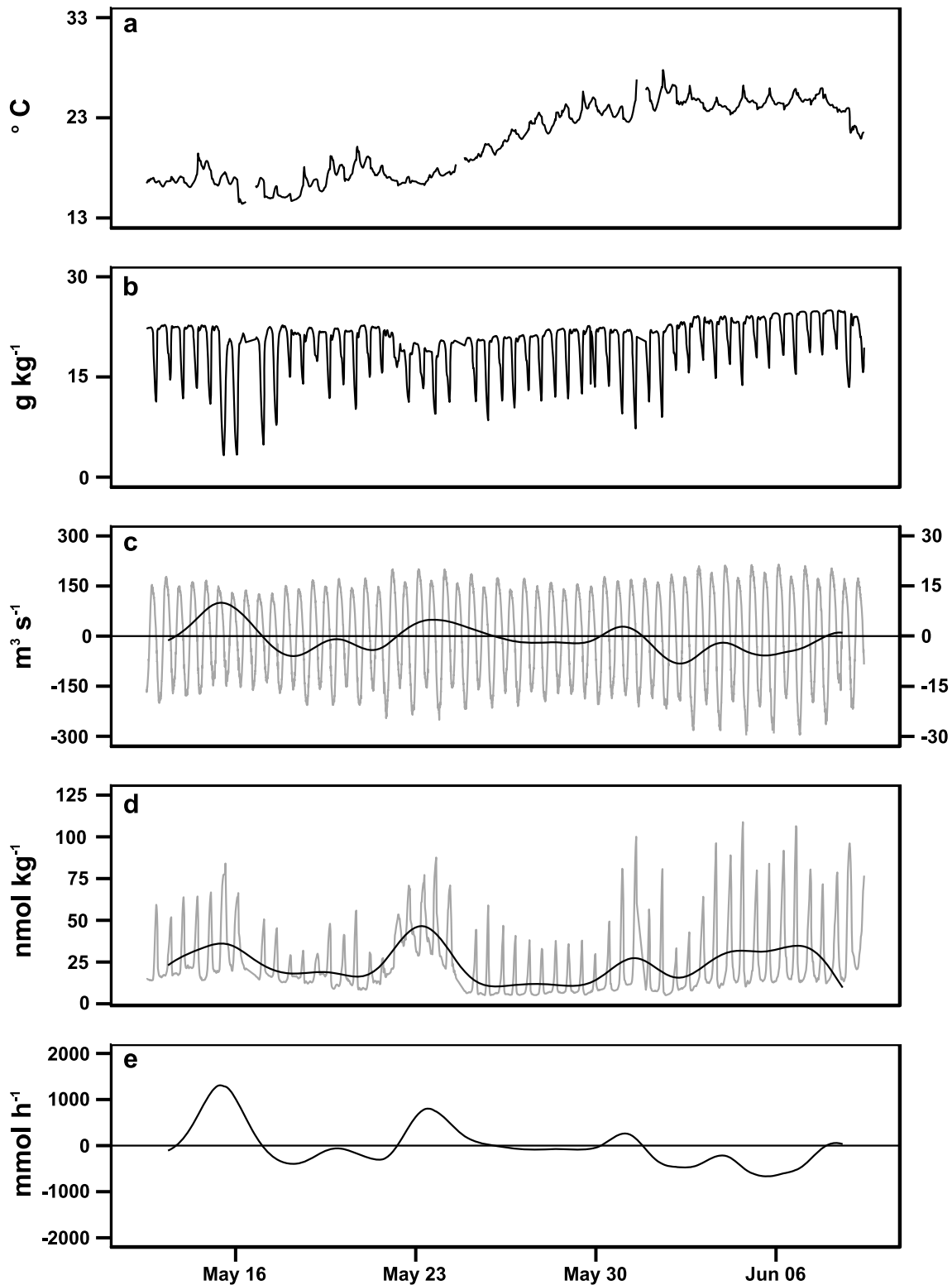

Fig. 3. Illustration of flux calculations using the product of discharge (Q, red) and proton concentration ($[H_T^+]$, blue) to determine instantaneous proton fluxes (H^+ Flux, purple). Positive values for discharge and flux indicate downstream flow, with negative values indicating upstream flow. Note that this illustration depicts an unfiltered flux to demonstrate the influence of tidal harmonics. The seasonal fluxes reported in this paper are filtered to remove these influences. (For interpretation of the references to colour in this figure legend, the reader is referred to the Web version of this article.)

sensor deployment and calibration procedures (Bresnahan et al. 2014; Gonski et al. 2018; Miller et al. 2018), [H$_T^+$] (nmol kg^{-1}) and fluxes (mmol h^{-1}) within and between physically dynamic estuarine and marine environments can now be reliably determined with high temporal

resolution and in the same manner as the fluxes of other dissolved constituents (for an illustrated demonstration of flux calculation see Fig. 3).

The combination of tidal forcing and biogeochemical processes with

Fig. 4. Raw and filtered time series data showing exchange between the Murderkill Estuary and Delaware Bay at Bowers Delaware during Spring of 2016. Time series of (a) temperature, (b) salinity, (c) discharge, (d) proton concentrations and (e) proton fluxes. Both the original data (grey line in c & d) and the non-tidal components (black line in c & d) of the original data, filtered using a low-pass Butterworth filter, are shown for discharge and protons. Proton fluxes were calculated from the non-tidal component of discharge and protons. Positive discharges and fluxes are directed downstream toward Delaware Bay.

respect to sampling date and time can both influence measured $[H_T^+]$ and our understanding of proton dynamics (Hofmann et al. 2009; Ullman et al. 2013). A conceptualization of the short-term variability in $[H_T^+]$ due to tidal forcing and its influence on conclusions drawn from lower frequency sampling is shown in Fig. 2. Proton concentrations from the Spring dataset were randomly sampled, means computed and the frequency distribution of 10,000 iterations plotted against the overall mean for the Spring (see Methods). An example of this random sampling shows that the extent to which $[H_T^+]$ variability due to tidal forcing is missed with less frequent samplings (Fig. 2a and b, orange and purple points). The frequency distributions show, even in this simple example, that sampling strategy can significantly affect the mean of measured $[H_T^+]$ and highlight the need for high frequency monitoring to truly understand acidification in these dynamic systems (Fig. 2c). Similar and more in-depth comparisons of the sample frequency for water quality monitoring show similar patterns (Skeffington et al. 2015; Gonski et al. 2018; Chappell et al. 2017; Miller et al. 2018). However, our subsampling does show that prior knowledge of the high frequency dynamics of $[H_T^+]$ over time might allow for a lower frequency sampling strategy that approximates the means obtained from higher frequency monitoring (Fig. 2c).

3.2. Proton fluxes through the Murderkill

Mean non-tidal proton fluxes were calculated for the two seasonal periods using the time series of low-pass filtered, instantaneous proton concentration and discharge measured at the mouth of the Murderkill River. We use the term "non-tidal" because filtering removes the influence of tidal variability and represents the net flux of protons upstream or downstream (see Methods). Instantaneous non-tidal proton fluxes ranged from -0.71 to 1.4 mmol h^{-1} in the Spring, and from -0.57 to 0.6 mmol h^{-1} in the Summer (Figs. 4 and 5), where positive flow is downstream. As a result, the Estuary's average upstream proton flux decreased by over 7-fold from the Spring (-9.6 ± 5.5 mmol h^{-1}) to the Summer (-1.3 ± 2.8 mmol h^{-1}; Table 1). A portion of this seasonal decrease is likely related to changes in non-tidal discharge during a drier Spring 2016 (total precipitation to the Murderkill was ~30 mm lower, data not shown), leading to less freshwater and proton input into the Estuary and a larger upstream recharge due to tidal forcing (Table 1). In addition to discharge, changes in the magnitude of proton-producing processes (e.g., respiration and nitrification), and proton-consuming processes (e.g., primary production and CO_2 degassing) will also influence proton cycling and the flux of protons (Cai et al. 2000; Wang and Cai, 2004; Hofmann et al. 2009).

The proton fluxes calculated here correspond surprisingly well with those modeled by Hofmann et al. for the Scheldt Estuary (2009). Although the Scheldt is much larger than the Murderkill Estuary and differs in its history and magnitude of human impacts, both systems are temperate, coastal plain estuaries that are turbid and nutrient-rich, and contain extensive salt marshes and mudflats (De Vriend et al. 2001; Ullman et al. 2013). While Hofmann and colleagues modeled *in situ* proton production and consumption, as opposed to the proton fluxes, the results are comparable. Summing the yearly consumption/production rates across their modeled boxes yields a net consumption of protons (increase in pH_T) that ranged from -0.03 kmol yr^{-1} ~100 km upstream to -0.40 kmol yr^{-1} at the mouth of the Estuary. Extrapolating our hourly to yearly fluxes gives a range of -0.08 kmol yr^{-1} to -0.01 kmol yr^{-1} using 12 months of either Spring or Summer rates, respectively. This annual flux is only an order of magnitude lower than that calculated for the mouth of the Scheldt Estuary, despite the Murderkill watershed being approximately two orders of magnitude smaller. Additional analyses over an entire year are clearly needed to provide a true annual flux for the Murderkill Estuary; however, it is encouraging that our calculated fluxes align with modeled values for another eutrophic, coastal plain estuary.

Our flux calculations demonstrate that the Murderkill Estuary

transports protons downstream and contributes to the acidification of Delaware Bay, but only for short periods of time (hours to days). Over longer periods, the Estuary acts as a sink for protons coming from the Bay and coastal ocean, likely driven by alkalinity generated during anaerobic respiration in marsh sediments (Ullman et al. 2013; Wang and Cai, 2004). The Murderkill Estuary discharges ~39 km upstream of the Bay's mouth and lies within a region where pH is highest in the Bay (Joesoef et al. 2017). Nutrient transport down the Murderkill stimulates phytoplankton productivity in the Bay (Voynova et al. 2015), thus reducing DIC and elevating pH. Other rivers discharge within this region of Delaware Bay (including the St. Jones, Mispillion Rivers and Cedar Creek in Delaware and the Maurice River in New Jersey), and may all contribute to the observed spike in pH. Similar to the proton flux, the pH within the Bay shows seasonal variation related to meteorological events, and biogeochemical processes within the watershed (Joesoef et al. 2017). If freshwater discharge has the largest impact on the long-term trend of $[H_T^+]$ in the Murderkill (e.g., Hofmann et al. 2009), it will be interesting to see how proton fluxes change over the course of a year and if the Estuary is truly a net sink for protons. These analyses will reveal the buffering effect of the Murderkill Estuary, along with other nearby estuaries, on Delaware Bay and the coastal ocean.
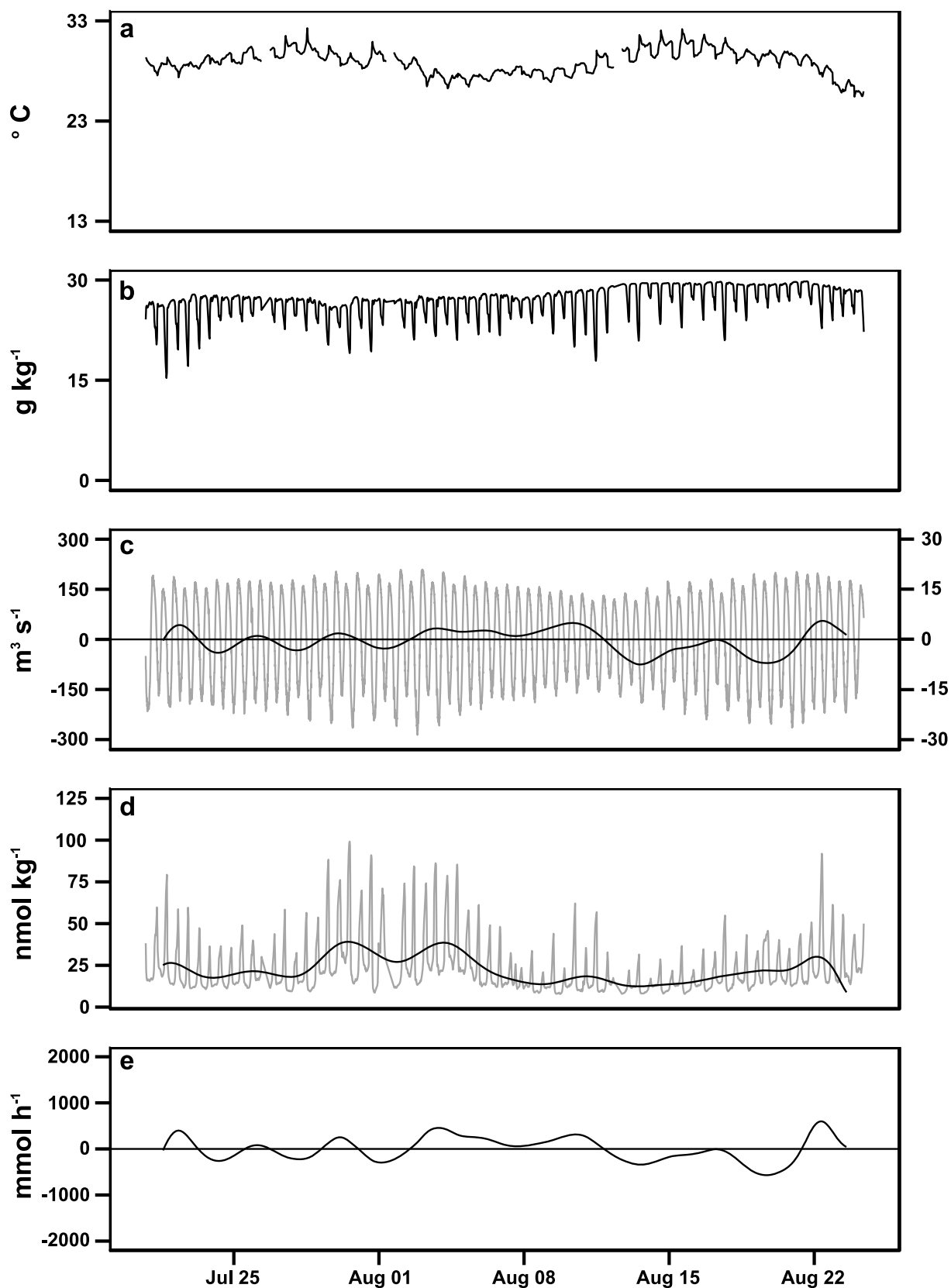
3.3. Tidal and seasonal changes in proton concentrations

Daily and seasonal variations in the pH of estuaries, bays and coastal oceans have been fairly well documented (e.g., Wang and Cai, 2004; Hofmann et al. 2011; Kline et al. 2015; Rivest and Gouhier, 2015; Takeshita et al. 2015; Wang et al. 2016), including Delaware Bay (Joesoef et al. 2017; Gonski et al. 2018). Proton concentrations at the mouth of the Murderkill River tracks tidal advection and, therefore, is inversely related to tidal cycle and salinity (Fig. 2a and b). The lowest $[H_T^+]$ (highest pH_T) occurs during flood tides when saline Delaware Bay water flows into the lower Murderkill Estuary. As the tide ebbs, $[H_T^+]$ increases (pH_T decreases) and reaches a maximum during the slack-low tide. In contrast to the flood tide, which produces a prolonged minimum in $[H_T^+]$, concentrations peak for only a short period of time (typically less than an hour) at slack ebb tide.

Respiration (a proton source) and primary production (a proton sink) are tidally coupled between the Murderkill Estuary and Delaware Bay, and contribute to the patterns described above (Voynova et al. 2015). Nutrients and DIC are transferred downstream and fuel primary productivity, the products of which (reactive organic matter) are subsequently transferred back upstream and fuel respiration (Wang and Cai, 2004; Voynova et al. 2015). Therefore, lower salinity waters discharging from the Murderkill Watershed (and to a lesser extent the wastewater treatment plant) are characterized by higher turbidity, undersaturated levels of dissolved O_2 and elevated DIC associated with net respiration and the production of protons (Ullman et al. 2013; Voynova et al. 2015). In contrast, higher salinity waters have elevated chlorophyll and O_2 concentrations (often supersaturated) associated with net primary production and the consumption of protons, typically occurring at the mouth of the Estuary and the margins of the Bay (Voynova et al. 2015). In other salt marsh ecosystems, additional processes such as CO_2 degassing and nitrification also play a large role in proton cycling, but the rates of these processes remain uncharacterized in this system (Hofmann et al., 2009; Jiang et al., 2008).

The respiration of organic matter produces both TA and DIC, and directly impacts the buffering capacity of natural waters (Wang and Cai, 2004). As DIC approaches equality with TA, buffering is reduced and waters are more susceptible to large changes in pH (Cai et al., 2011). While mean $[H_T^+]$ were similar in the Spring (24.6 nmol $kg^{-1} \pm 0.2$ S.E.) and Summer (22.8 nmol $kg^{-1} \pm 0.2$ S.E.), a sampling of TA and DIC over a Spring and Summer tidal cycle shows the processes controlling proton cycling differ between the seasons (Fig. 6). The elevated concentrations of TA and DIC during the Summer ebb tide, relative to the Spring, are

Fig. 5. Raw and filtered time series data showing exchange between the Murderkill Estuary and Delaware Bay at Bowers Delaware during Summer of 2016. Time series of (a) temperature, (b) salinity, (c) discharge, (d) proton concentrations and (e) proton fluxes. Both the original data (grey line in c & d) and the non-tidal components (black line in c & d) of the original data, filtered using a low-pass Butterworth filter, are shown for discharge and protons. Proton fluxes were calculated from the non-tidal component of discharge and protons. Positive discharges and fluxes are directed downstream toward Delaware Bay.
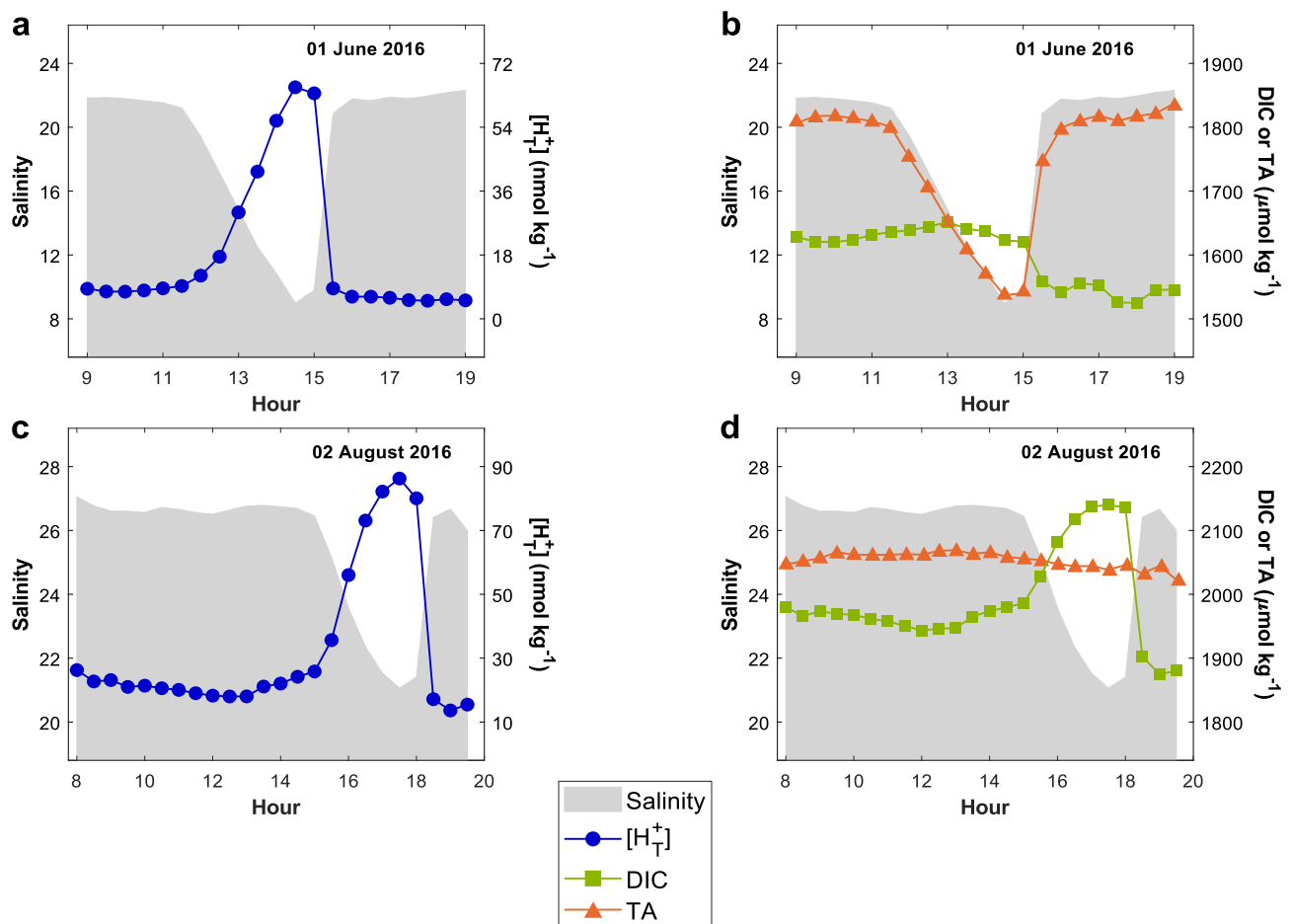
consistent with the export of both constituents from the surrounding salt marshes due to the respiration of accumulated organic matter. Salt marshes surrounding the lower Murderkill are a sink for organic matter and, as such, these marshes contribute both TA and DIC to the Estuary that vary seasonally and affect the waters' buffering capacity (Wang and Cai, 2004; Sharp, 2011; Ullman et al. 2013; Wang et al. 2016). The reactive organic matter that likely drives proton production and cycling in the Murderkill River is a mixture of marine and freshwater (upper watershed cyanobacterial blooms) phytoplankton, vascular plant detritus, and suspended sedimentary particles (Ullman et al. 2013; Andres et al. 2019). Variations in these sources over time ultimately influence net watershed respiration, and thus [H_T^+], beyond that of non-tidal mean discharge alone (Voynova et al. 2015). More research is underway to better understand the magnitude of organic matter respiration, along with other biogeochemical processes and meteorological phenomenon, on proton production and transport within the Murderkill Estuary.

3.4. Strengths and limitations of the proton flux method

The proton flux method is not exclusive of other, more established methods for characterizing the acidification of estuaries and coastal waters. But rather, is another tool in the toolbox to disentangle the complexities of acidification that include processes such as the absorption of anthropogenic CO_2, net community production, calcification, and air-sea gas exchange, among numerous other factors. The present methodology provides a novel way of using physical forcing (discharge)

to scale down from regional to local influences (and vice versa) to assess the magnitude of proton dynamics in smaller systems and to resolve how these dynamics may buffer or further acidify larger systems. The present case study clearly demonstrates that further acidification or buffering can occur as a result of inter-system interactions and exchange within the freshwater-influenced Delaware Bay-Murderkill Estuary system, dynamics that existing methods for the study and modeling of nearshore acidification may fail to accurately estimate or include (Kwiatkowski and Orr, 2018). Models are only as good as the data that feeds them. If the models only capture constant and idealized variability in tidal signals and exchange, then past approaches to the study of estuarine and coastal acidification may result in substantial and/or disproportionate error in extrapolating from present to future acidification trends and dynamics.

The proton flux method ultimately captures and integrates the real, *in situ* variability representative of estuarine processes. In addition to the astronomical variability in tidal cycles (e.g., neap vs. spring tides), the balance between freshwater discharge and tidal forcing changes over time. Variability also influences calculated metrics like the Revelle Factor which describes the dynamic ability of the global oceans to absorb atmospheric CO_2 and remains a key characteristic for estimating acidification based on the oceanic uptake of anthropogenic carbon (Carter et al. 2019; Egleston et al. 2010). Variability in tides and discharge also affects the carbonate system by altering rates of dilution and buffering capacity, and the proton flux method allows researchers to integrate this variability into their methods and analyses. In addition, the method incorporates not only high temporal variability, but

Fig. 6. Tidal dynamics of [H_T^+] (blue circles, a & c), DIC (green squares, b & d) and TA (orange triangles, b & d) with respect to salinity (solid grey) for a Spring (a, b) and Summer (c, d) sampling of a full tidal cycle. Discrete samples were taken every half-hour for DIC and TA, while salinity and [H_T^+] were measured by the SeapHOx sensor at the same interval. (For interpretation of the references to colour in this figure legend, the reader is referred to the Web version of this article.)

indirectly, spatial variability by sampling the waters from two different end-members over the course of a tidal cycle.

The proton flux method provides advantages over other approaches, but it is not without its limitations. The method reveals the net result of proton cycling and the upstream or downstream proton sources and sinks, but it does not identify the specific processes (e.g., primary production or anaerobic respiration) that produce and consume protons. Additional sampling of other parameters is needed to define and quantify the rates of these component processes. Similarly, there is still a need to calibrate the pH sensors by measuring marine CO_2 system parameters (DIC and TA in this study) in the field, so the method is not exclusive of other methods that examine acidification. Discharge measurements are also needed, which may limit the use of this method in some locations. The mouth of the Murderkill Estuary is a well-mixed system, so the data presented here represents the entire water column. Using the proton flux method in stratified water columns would require additional resources, but is still feasible. For example, additional monitoring that included depth profiling or the use of multiple sensors could account for differential proton cycling occurring in the various, vertically stratified water masses.

4. Conclusions and the future of proton fluxes

The present work demonstrates the tidal and non-tidal dynamics of $[H_T^+]$ in an estuarine ecosystem. Using continuous, high frequency monitoring to track proton concentrations, together with discharge measurements, we can now precisely quantify the upstream and downstream fluxes of protons and the net direction of coastal acidification (i.e., sources vs. sinks). The Murderkill Estuary was used as a case study to demonstrate this novel way of characterizing acidification of nearshore waters, and show temporal changes, from minutes to months, in the magnitude and direction of acidification. Including the proton flux method together with a complementary approach that combines advanced time series analyses and proton modeling using concentrations measured at high-frequency as model inputs and validation can provide a powerful technique to resolve current estuarine acidification mechanisms and trends (Hofmann et al. 2009, Fassbender et al. 2017, -Feely et al., 2018; Kwiatkowski and Orr, 2018, Miller et al. 2018, Pacella et al., 2018). With the appropriate sensors, similar monitoring and analyses can be performed in any free-flowing freshwater, estuarine or marine system and provides one more tool to identify those water bodies that are receiving elevated $[H_T^+]$, and may be more vulnerable to future acidification.

Proton concentration, or pH, is known as a "master" variable of aquatic biogeochemistry because it is both affected by and governs so many processes (Stumm and Morgan, 1996). As such, proton cycling is a more appropriate way to view and quantify estuarine and coastal acidification (Hofmann et al. 2010; Fassbender et al. 2017; Kwiatkowski and Orr, 2018). Proton concentrations are a more robust environmental indicator of acidification than pH because changes in pH are related not only to proton concentration, but also the initial pH of the water body and its temperature- and salinity-dependent buffer capacity (Fassbender et al. 2017). The present work is meant to stimulate additional discussion already occurring in the literature on the way researchers measure and characterize the acidification of natural waters by moving towards the direct measurement, reporting and analysis of proton concentrations, in addition to pH and other marine CO_2 system parameters (e.g., Hofmann et al. 2010; Fassbender et al. 2017; Kwiatkowski and Orr, 2018). The precise controls of proton production and consumption are not, as yet, known for the Murderkill Estuary. However, the tools presented here will provide the basis for further studies to improve our mechanistic understanding of the processes that drive proton production, consumption, and transport within this and other systems, and when used in conjunction with other established methods will provide a better understanding of the sensitivity of nearshore waters to current and future acidification.

Author contributions

The manuscript was written through contributions of all authors. All authors have given approval to the final version of the manuscript.

Declaration of competing interest

There are no conflicts of interest.

References

Andres, A.S., 2004. Ground-water Recharge Potential Mapping in Kent and Sussex Counties, Delaware. Report of Investigations 66. Delaware Geological Survey, Newark, DE, p. 20.

Andres, A.S., Main, C.R., Pettay, D.T., Ullman, W.J., 2019. Hydrological controls of cyanobacterial blooms in Coursey Pond, Delaware (USA). J. Environ. Qual. 48, 73–82.

Aufdenkampe, A.K., Mayorga, E., Raymond, P.A., Melack, J.M., Doney, S.C., Alin, S.A., Aalto, R.E., Yoo, K., 2011. Riverine coupling of biogeochemical cycles between land, oceans, and the atmosphere. Front. Ecol. Environ. 9 (1), 53–60.

Bates, R.G., 1973, 2ed. Determination of pH: Theory and Practice. Wiley-Interscience.

Bates, N.R., Astor, Y.M., Church, M.J., Currie, K., Dore, J.E., Gonzalez-Davila, M., Lorenzoni, L., Muller-Karger, F., Olafsson, J., Santana-Casino, J.M., 2014. A Time-Series View of Changing Surface Ocean Chemistry Due to Ocean Uptake of Anthropogenic CO_2 and Ocean Acidification. Oceanography 27, 126–141.

Borges, A.V., Gypens, N., 2010. Carbonate chemistry in the coastal zone responds more strongly to eutrophication than to ocean acidification. Limnol. Oceanogr. 55, 346–353.

Bresnahan Jr., P.J., Martz, T.R., Takeshita, Y., Johnson, K.S., LaShomb, M., 2014. Best practices for autonomous measurement of seawater pH with the Honeywell Durafet. Methods. Oceanogr. 9, 44–60.

Butler, R.A., Covington, A.K., Whitfield, M., 1985. The determination of pH in estuarine waters. II: practical considerations. Oceanol. Acta 8 (4), 433–439.

Cai, W.-J., Hu, X., Huang, W.-J., Jiang, L.-Q., Wang, Y., Peng, T.-H., Zhang, X., 2010. Alkalinity distributions in the western north atlantic ocean margins. J. Geophys. Res.: Oceans 115, 1–15.

Cai, W.-J., Hu, X., Huang, W.-J., Murrell, M.C., Lehrter, J.C., Lohrenz, S.E., Chou, W.-C., Zhai, W., Hollibaugh, J.T., Wang, Y., Zhao, P., Guo, X., Gundersen, K., Dai, M., Gong, G.-C., 2011. Acidification of subsurface coastal waters enhanced by eutrophication. Nat. Geosci. 23, 766–770.

Cai, W.-J., Wang, Y., 1998. The chemistry, fluxes, and sources of carbon dioxide in the estuarine waters of the Satilla and Altamaha Rivers, Georgia. Limnol. Oceanogr. 43 (4), 657–668.

Cai, W.-J., Wiebe, W.J., Wang, Y., Sheldon, J.E., 2000. Intertidal marsh as a source of dissolved inorganic carbon and a sink of nitrate in the Satilla River-estuarine complex in the southeastern U.S. Limnol. Oceanogr. 8, 1743–1752.

Carstensen, J., Duarte, C.M., 2019. Drivers of pH variability in coastal ecosystems. Environ. Sci. Technol. 53 (8), 4020–4029.

Carter, B.R., Feely, R.A., Wanninkhof, R., Kouketsu, S., Sonnerup, R.E., Pardo, P.C., Sabine, C.L., Johnson, G.C., Sloyan, B.M., Murata, A., Mecking, S., Tilbrook, B., Speer, K., Talley, L.D., Millero, F.J., Wijffels, S.E., Macdonald, A.M., Gruber, N., Bullister, J.L., 2019. Pacific anthropogenic carbon between 1991 and 2017. Global Biogeochem. Cycles 33 (5), 597–617.

Chappell, N.A., Jones, T.D., Tych, W., 2017. Sampling frequency for water quality variables in streams: systems analysis to quantify minimum monitoring rates. Water Res. 123, 49–57.

Dickson, A.G., 1984. pH scales and proton-transfer reactions in saline media such as sea water. Geochem. Cosmochim. Acta 48, 2299–2308.

Dickson, A.G., 1990. Standard potential of the reaction: AgCl (s) + 1/2 H$_2$ (g) = Ag (s) + HCl (aq), and the standard acidity constant of the ion HSO$_4^-$ in synthetic sea water from 273.15 to 318.15 K. J. Chem. Therm. 22 (2), 113–127.

Dickson, A.G., 1993. The measurement of seawater pH. Mar. Chem. 44, 131–142.

DNREC, 2006. Technical Analysis for the Proposed Murderkill River Bacteria TMDL. Delaware Department of Natural Resources and Environmental Control, Dover, p. 35.

DNREC, 2014. Murderkill river watershed revised nutrient and dissolved oxygen TMDLs. Delaware Department of Natural Resources and Environmental Control, Dover.

Duarte, C.M., Hendriks, I.E., Moore, T.S., Olsen, Y.S., Steckbauer, A., Ramajo, L., Carstensen, J., Trotter, J.A., McCulloch, M., 2013. Is ocean acidification an open-ocean syndrome? Understanding anthropogenic impacts on seawater pH. Estuar. Coast 36, 221–236.

Dzwonkowski, B., Wong, K.C., Ullman, W.J., 2014. Water level and velocity characteristics of a salt marsh channel in the Murderkill Estuary, Delaware. J. Coast Res. 30, 63–74.

Easley, R.A., Byrne, R.H., 2012. Spectrophotometric calibration of pH electrodes in seawater using purified m-Cresol Purple. Environ. Sci. Technol. 46 (9), 5018–5024.

Egleston, E.S., Sabine, C.L., Morel, F.M., 2010. Revelle revisited: buffer factors that quantify the response of ocean chemistry to changes in DIC and alkalinity. Global Biogeochem. Cycles 24 (1).

Fassbender, A.J., Alin, S.R., Feely, R.A., Sutton, A.J., Newton, J., Krembs, C., et al., 2018a. Seasonal carbonate chemistry variability in marine surface waters of the Pacific Northwest. Earth Syst. Sci. Data 10, 1367–1401. https://doi.org/10.1371/journal.pone.0089619.

Fassbender, A.J., Rodgers, K.B., Palevsky, H.I., Sabine, C.L., 2018b. Seasonal asymmetry in the evolution of surface ocean pCO$_2$ and pH thermodynamic drivers and the influence on sea-air CO2 flux. Global Biogeochem. Cycles 32, 1476–1497.

Fassbender, A.J., Sabine, C.L., Palevsky, H.I., 2017. Nonuniform ocean acidification and attenuation of the ocean carbon sink. Geophys. Res. Lett. 44 (16), 8404–8413.

Feely, R.A., Alin, S.R., Newton, J., Sabine, C.L., Warner, M., Devol, A., Krembs, C., Maloy, C., 2010. The combined effects of ocean acidification, mixing, and respiration on pH and carbonate saturation in an urbanized estuary. Estuar. Coast Shelf Sci. 88, 442–449.

Feely, R.A., Okazaki, R.R., Cai, W.J., Bednaršek, N., Alin, S.R., Byrne, R.H., Fassbender, A., 2018. The combined effects of acidification and hypoxia on pH and aragonite saturation in the coastal waters of the California current ecosystem and the northern Gulf of Mexico. Continental Shelf Research 152, 50–60.

Ganju, N.K., Schoellhamer, D.H., Bergamaschi, B.A., 2005. Suspended sediment fluxes in a tidal wetland: measurement, controlling factors, and error analysis. Estuaries 28, 812–822.

Gonski, S.F., Cai, W.-J., Ullman, W.J., Joesoef, A., Main, C.R., Pettay, D.T., Martz, T.R., 2018. Assessment of the suitability of Durafet-based sensors for pH measurement in dynamic estuarine environments. Estuar. Coast Shelf Sci. 200, 152–168.

Gran, G., 1950. Determination of the equivalence point in potentiometric titrations. Acta Chem. Scand. 4, 559–577.

Gran, G., 1952. Determination of the equivalence point in potentiometric titrations–Part II. Analyst 77 (920), 661–671.

Hofmann, A.F., Meysman, F.J.R., Soetaert, K., Middelburg, J.J., 2008. A step-by-step procedure for pH model construction in aquatic systems. Biogeosciences 5, 227–251.

Hofmann, A.F., Middelburg, J.J., Soetaert, K., Meysman, F.J.R., 2009. pH modelling in aquatic systems with time-variable acid-base dissociation constants applied to the turbid, tidal Scheldt estuary. Biogeosciences 6, 1539–1561.

Hofmann, A.F., Middelburg, J.J., Soetaert, K., Wolf-Gladow, D.A., Meysman, F.J.R., 2010. Proton Cycling, buffering, and reaction stoichiometry in natural waters. Mar. Chem. 121, 246–255.

Hofmann, G.E., Smith, J.E., Johnson, K.S., Send, U., Levin, L.A., Micheli, F., Paytan, A., Price, N.N., Peterson, B., Takeshita, Y., Matson, P.G., Derse-Crook, E., Kroeker, K.J., Gambi, M., Rivest, E.B., Frieder, C.A., Yu, P.C., Martz, T.R., 2011. High-frequency dynamics of ocean pH: a multi-ecosystem comparison. PloS One 6 (12).

Huang, W.-J., Wang, Y., Cai, W.-J., 2012. Assessment of sample storage techniques for total alkalinity and dissolved inorganic carbon in seawater. Limnol Oceanogr. Methods 10 (9), 711–717.

Jiang, L.-Q., Cai, W.-J., Wannikhoff, R., Wang, Y., Luger, H., 2008. Air-sea CO2 fluxes on the US South Atlantic Bight: spatial and seasonal variability. Journal of Geophysical Research: Oceans (1978-2012) 113.

Joesoef, A., Kirchman, D.L., Sommerfield, C.K., Cai, W.-J., 2017. Seasonal variability of the inorganic carbon system in a large coastal plain estuary. Biogeosciences 14, 4949–4963.

Jokiel, P.L., 2016. Predicting the impact of ocean acidification on coral reefs: evaluating the assumptions involved. J. Mar. Sci. 73 (3), 550–557.

Kline, D.I., Teneva, L., Hauri, C., Schneider, K., Miard, T., Chai, A., et al., 2015. Six month in situ high-resolution carbonate chemistry and temperature study on a coral reef flat reveals asynchronous pH and temperature anomalies. PloS One 10 (6), e0127648.

Kwiatkowski, L., Orr, J.C., 2018. Diverging seasonal extremes for ocean acidification during the twenty-first century. Nat. Clim. Change 8 (2), 141.

Lee, K., Kim, T.-W., Byrne, R.H., Millero, F.J., Feely, R.A., Liu, Y.-M., 2010. The universal ratio of boron to chlorinity for the North Pacific and North Atlantic oceans. Geochem. Cosmochim. Acta 74 (6), 1801–1811.

Ligges, U., et al., 2013. signal: signal processing. URL: http://r-forge.r-project.org/projects/signal/.

Martz, T.R., Connery, J.G., Johnson, K.S., 2010. Testing the Honeywell Durafet® for seawater pH applications. Limnol Oceanogr. Methods 8, 172–184.

Millero, F.J., Graham, T.B., Huang, F., Bustos-Serrano, H., Pierrot, D., 2006. Dissociation constants of carbonic acid in seawater as a function of salinity and temperature. Mar. Chem. 100 (1), 80–94.

Miller, C.A., Pocock, K., Evans, W., Kelley, K.L., 2018. An evaluation of the performance of Sea-Bird Scientific's SeaFET autonomous pH sensor: considerations for the broader oceanographic community. Ocean Sci. 14, 751–768.

Martz, T.R., Daly, K.L., Byrne, R.H., Stillman, J.H., Turk, D., 2015. Technology for ocean acidification research: needs and availability. Oceanography 28 (2), 40–47.

Newton, J.A., Feely, R.A., Jewett, E.B., Williamson, P., Mathis, J., 2015. Global Ocean Acidification Observing Network: Requirement and Governance Plan, second ed. GOA-ON.

Pacella, S.R., Brown, C.A., Waldbusser, G.G., Labiosa, R.G., Hales, B., 2018. Seagrass habitat metabolism increases short-term extremes and long-term offset of CO$_2$ under future ocean acidification. Proceedings of the National Academy of Sciences U.S.A. 115, 3870–3875.

Pierrot, D., Lewis, E., Wallace, D.W.R., 2006. CO2SYS DOS Program Developed for CO$_2$ System Calculations. ORNL/CDIAC-105, Carbon Dioxide Information Analysis Center. Oak Ridge National Laboratory, US Department of Energy, Oak Ridge, TN.

Provoost, P., Van Heuven, S., Soetaert, K., Laane, R.W.P.M., Middelburg, J.J., 2010. Seasonal and long-term changes in pH in the Dutch coastal zone. Biogeosciences 7 (11), 3869.

Rivest, E.B., Gouhier, T.C., 2015. Complex environmental forcing across the biogeographical range of coral populations. PloS One 10 (3), e0121742.

Sharp, J.H., 2011. Primary production in the Murderkill River. A report to kent county and Delaware DNREC. Unpublished Report: http://www.dnrec.delaware.gov/swc/wa/Documents/WAS/Murderkill%20River%20Reports/New%20Murderkill%20Page/1.%20Primary%20Production%20Study%20Report.pdf.

Skeffington, R.A., Halliday, S.J., Wade, A.J., Bowes, M.J., Loewenthal, M., 2015. Using high-frequency water quality data to assess sampling strategies for the EU Water Framework Directive. Hydrol. Earth Syst. Sci. 19, 2491–2504.

Stumm, W., Morgan, J.J., 1996. Aquatic Chemistry: Chemical Equilibria and Rates in Natural Waters, third ed. Wiley-Interscience.

Sunda, W.G., Cai, W.J., 2012. Eutrophication induced CO2 –Acidification of subsurface coastal waters: interactive effects of temperature, Salinity, and pCO$_2$. Environ. Sci. Technol. 46, 10651–10659.

Takeshita, Y., Frieder, C.A., Martz, T.R., Ballard, J.R., Feely, R.A., Kram, S., Nam, S., Navarro, M.O., Price, N.N., Smith, J.E., 2015. Including high-frequency variability in coastal ocean acidification projections. Biogeosciences 12, 5853–5870.

Takeshita, Y., Martz, T.R., Johnson, K.S., Dickson, A.G., 2014. Characterization of an ion-selective field effect transistor and chloride ion-selective electrodes for pH measurements in seawater. Anal. Chem. 86 (22), 1189–1195.

Ullman, W.J., Aufdenkampe, A., Hays, R.L., Dix, S., 2013. Nutrient Exchange between a Salt Marsh and the Murderkill Estuary, Kent County, Delaware. Part C. Technical Report. Delaware Department of Natural Resources and Environmental Control, Dover, DE. Unpublished Report. http://www.dnrec.delaware.gov/swc/wa/Documents/WAS/Murderkill%20River%20Reports/New%20Murderkill%20Page/3.%20Study%20of%20Tidal%20Marsh%20Fluxes%20of%20Nutrients%20and%20DO.pdf.

Velinsky, D., Sommerfield, C., Charles, D., 2010. Vertical profiles of radioisotopes, nutrients, and diatoms in sediment cores from the tidal Murderkill River basin: a historical analysis of ecological change and sediment accretion. PCER Report 10-01. http://www.dnrec.delaware.gov/Admin/DelawareWetlands/Documents/Data%20Portal/ANSP%20Murderkill%20River%20Final%20Report%20see%20email%20from%20Chris%20B%20relating.pdf.

Voynova, Y.G., Lebaron, K.C., Barnes, R.T., Ullman, W.J., 2015. *In situ* response of bay productivity to nutrient loading from a small tributary: the Delaware Bay-Murderkill Estuary tidally-coupled biogeochemical reactor. Estuar. Coast Shelf Sci. 160, 33–48.

Voynova, Y.G., Sharp, J.H., 2012. Anomalous biogeochemical response to a flooding event in the Delaware Estuary: a possible typology shift due to climate change. Estuar. Coast 35, 943e958.

Wallace, R.B., Baumann, H., Grear, J.S., Aller, R.C., Gobler, C.J., 2014. Coastal Ocean Acidification: the other eutrophication problem. Estuar. Coast Shelf Sci. 148, 1–13.

Wang, Z.A., Cai, W.-J., 2004. Carbon dioxide degassing and inorganic carbon export from a marsh-dominated estuary (the Duplin River): a marsh CO$_2$ pump. Limnol. Oceanogr. 49, 314–354.

Wang, Z.A., Kroeger, K.D., Ganju, N.K., Gonneea, M.E., Chu, S.N., 2016. Intertidal salt marshes as an important source of inorganic carbon to the coastal ocean. Limnol. Oceanogr. 61, 1916–1931.

Whitfield, M., Bulter, R.A., Covington, A.K., 1985. The determination of pH in estuarine waters. I: definitions of pH scales and selection of buffers. Oceanol. Acta 8 (4), 423–432.

Wong, K.-C., Dzwonkowski, B., Ullman, W.J., 2009. Temporal and spatial variability of sea level and volume flux in the Murderkill Estuary. *Estuarine*. Coast Shelf Sci. 84, 440–446.

Wootton, J.T., Pfister, C.A., 2012. Carbon system measurements and potential climatic drivers at a site of rapidly declining ocean pH. PloS One 7 (12) e53396.